High-Symmetry DC SQUID Based on the Nb/AlO$_x$/Nb Josephson Junctions for Nondestructive Evaluation[1]

E. A. Kostyurina[a, b, *]**, K. V. Kalashnikov**[a, b]**, L. V. Filippenko**[a]**, O. S. Kiselev**[a]**, and V. P. Koshelets**[a]

[a]*Kotel'nikov Institute of Radio Engineering and Electronics, Russian Academy of Sciences, Moscow, 125009 Russia*

[b]*Moscow Institute of Physics and Technology (State University), Dolgoprudnyi, Moscow oblast, 141700 Russia*

***e-mail: kostyurina@hitech.cplire.ru**

Received June 21, 2017

Abstract—Topology of high-symmetry thin-film SQUIDs based on the Nb/AlO$_x$/Nb tunneling junctions is developed and optimized. The devices exhibit relatively low sensitivity to static external field and electric interference. An experimentally implemented SQUID sensor with an integrated input coil with a sensitivity of 0.26 μA/Φ$_0$ exhibits an intrinsic noise with respect to magnetic flux of less than $5\,\mu\Phi_0/\sqrt{\mathrm{Hz}}$. A system for encapsulation of sensors is developed for applications in multichannel systems for nondestructive evaluation of materials and alternative diagnostic systems.

INTRODUCTION

There has been considerable recent interest in the methods for detection of critical defects in various industrial items. Methods for nondestructive evaluation (NDE) are widely employed for detection, localization, and estimation of the parameters of defects in various metal objects or parts of such objects. Note the method based on the excitation of the Foucault currents and the subsequent analysis of the electromagnetic field that is generated by such currents using magnetometric systems based on SQUIDs, which are known to be the most sensitive sensors of magnetic field [1, 2]. A two-contact SQUID scheme is based on a superconducting ring with two Josephson junctions connected in parallel. The working principle of SQUID is based on the detection of output voltage V_{out} that is induced by the magnetic flux through the SQUID loop [3]. The development of Russian science and technology is aimed at import substitution which involves, in particular, the development and fabrication of low-noise SQUIDs. This work is devoted to the development of SQUIDs with an intrinsic noise with respect to magnetic flux of $1-10\,\mu\Phi_0/\sqrt{\mathrm{Hz}}$ that can be used in NDE systems.

1. DEVELOPMENT OF THE SQUID TOPOLOGY

A multichannel magnetometric system that can be used in several applications including NDE is being developed at the Kotel'nikov Institute of Radio Engineering and Electronics, Russian Academy of Sciences. The system is based on the SQUID magnetometer that allows measurements of fields with an induction of less than 10^{-10} G. The high-symmetry SQUID structure of [7, 8] (Fig. 1) is used to develop the SQUID magnetometer. The advantage of such a structure in comparison with the classical (washer) detectors [4−6] lies in the fact that the structure works as a first-order gradiometer with respect to magnetic field, so that the SQUID can be used outside a magnetically shielded room. In addition, the symmetry of bias currents makes it possible to eliminate the effect of interference on connecting wires.

A niobium film with a thickness of 150 nm serves as the electrode in the proposed SQUID. Four circular holes (two holes with a diameter of 40 μm and two holes with a diameter of 15 μm) are formed in the film. The holes are connected with slits that intersect at the center of the electrode at a right angle. Two larger (smaller) holes are inductively connected with the input (modulation) coils [3, 9].

The slit widths of 4 μm and lengths of 600 and 300 μm are optimal for the formation of the input and modulation coils with a sufficient number of turns that

---

[1] This work was awarded at the Anisimkin Contest for young scientists in 2016.
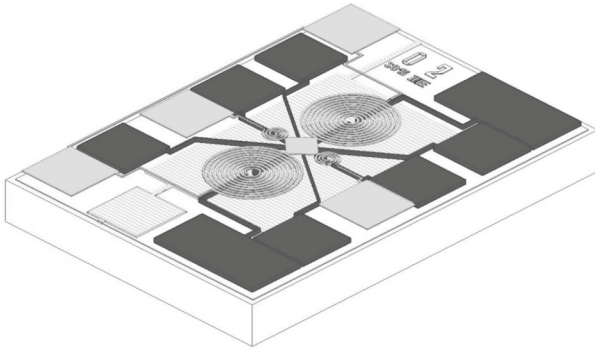
Fig. 1. Topology of the high-symmetry DC SQUID.

are symmetrically separated in space. Note also the absence of bending of the connecting lines. Two Josephson junctions with an area of $S = 1.5$ μm^2 are formed on the $Nb/AlO_x/Nb$ three-layer structure using the selective niobium etching and anodization process (SNEAP) [10] on different sides of the intersection of slits. To provide the hysteresis-free I–V characteristic, we shunt the junctions using molybdenum stripes with a total resistance of 5 Ω. To decrease

the SQUID inductance [4] and, hence, dimensionless inductance [3], we shield the slits with the aid of niobium stripes with a width of 30 μm located at a distance of 200 nm from the base electrode. Thus, the inductance is decreased by 60% to a level of about 90 pH.

Symmetric bias currents and, hence, insensitivity to magnetic fields induced by supply currents in connecting contacts (that may lead to an increase in the intrinsic noise of the sensor) are important advantages of the proposed SQUID topology. To verify the efficiency of the proposed method, we study the effect of bias currents on the SQUID characteristics. The voltage–flux characteristics are measured for asymmetric and symmetric power supply schemes (Figs. 2a and 2b) at several bias currents. The deviation of the SQUID voltage from the mean value at the given bias current is shown using shades of grey (light- and dark-grey colors correspond to the minimum and maximum values, respectively). The experiments with the asymmetric configuration that corresponds to the four-wire measurement scheme show that the shift of voltage–flux characteristics due to variation in the bias current corresponds to a SQUID sensitivity to the bias current of 40 μA/Φ_0 (Fig. 2c). As was expected, the dependence
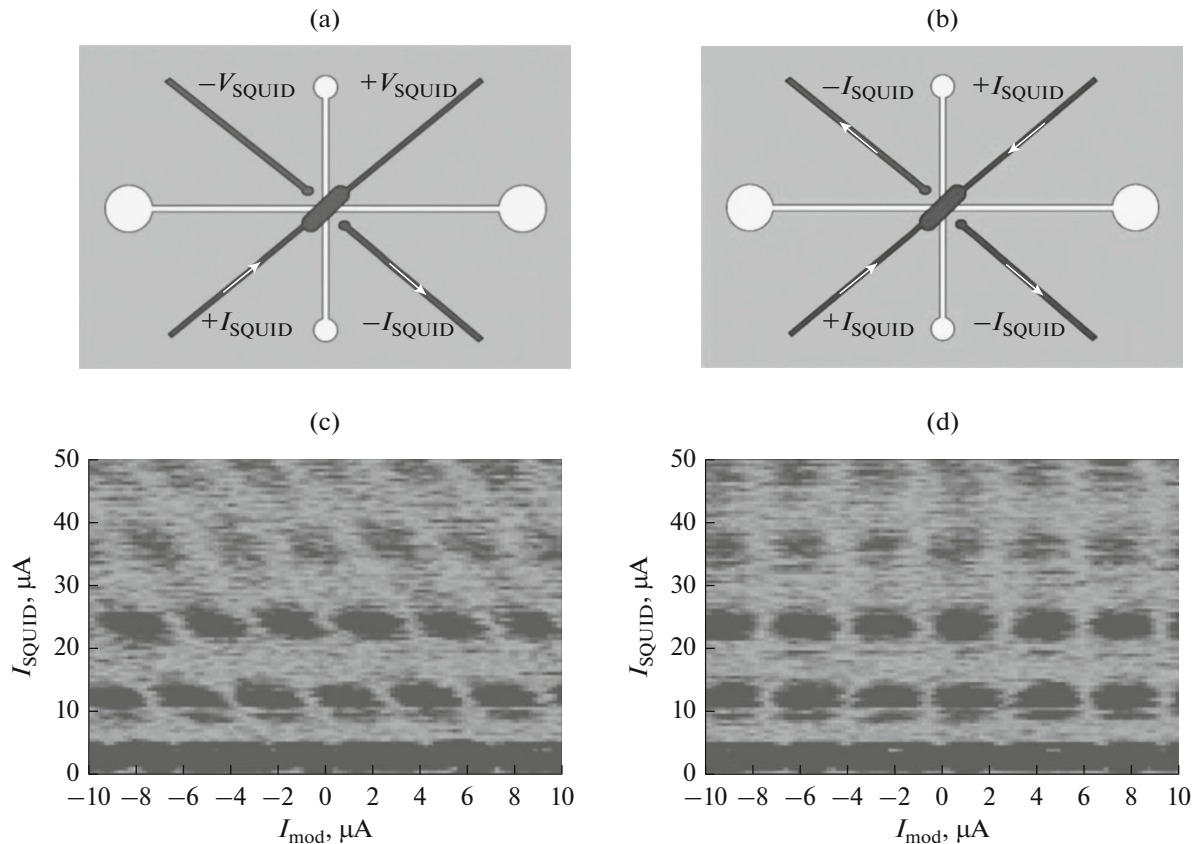

Fig. 2. Scheme of currents and measured voltages for (a) asymmetric and (b) symmetric configurations and plots of voltage–flux characteristics vs. bias current for (c) asymmetric and (d) symmetric schemes of the bias current.
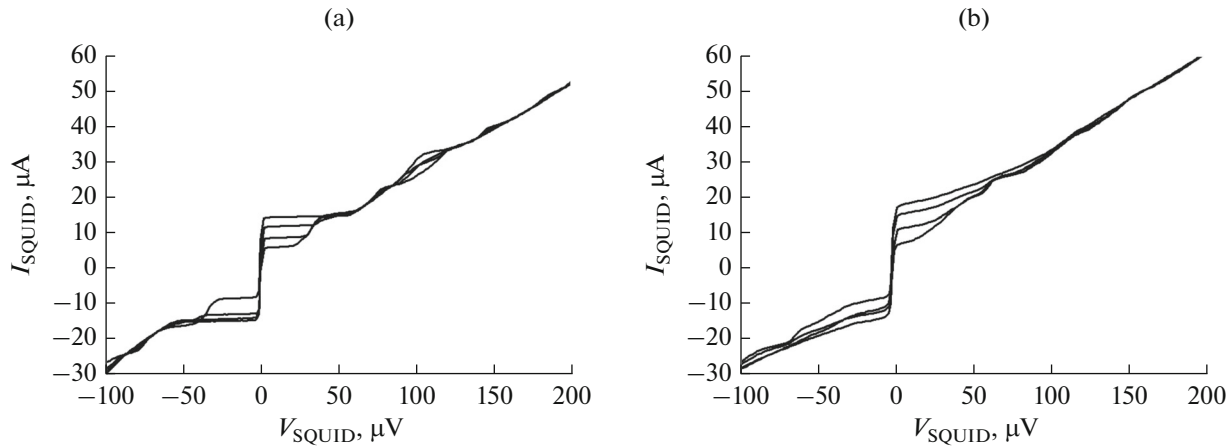
(a)

(b)

Fig. 3. Dependences of the $I-V$ characteristics of the SQUID on the magnetic flux through the SQUID for (a) nonoptimized and (b) optimized topology of the SQUID sensor.

of the extrema of the voltage−flux characteristics on the bias current vanishes for the symmetric configuration (Fig. 2d), so that the corresponding SQUID is insensitive to interference in the connecting lines.

The mutual inductance of the input and modulation coils decreases due to spatial separation of the coils by about 200 μm, and the direction of currents in the coils is chosen in such a way that the magnetic fluxes generated by the currents are pairwise contradirectional. The width of a turn is equal to the distance between the turns (2.5 and 5 μm for the input and modulation coils, respectively). The numbers of turns of the input and modulation coils are $N_i = 80$ and $N_m = 10$. The input sensitivity is 0.26 μA/Φ_0 for the input coils.

2. EXPERIMENTAL RESULTS AND OPTIMIZATION OF THE STRUCTURE

The $I-V$ characteristics of the above samples exhibit intervals of a relatively high differential resistance that correspond to resonances at frequencies of about 100 GHz resulting from the interaction of the Josephson oscillations and the electromagnetic fields in the vicinity of the junctions. The positions of such resonances correspond to the SQUID working region and lead to cutting of the $I-V$ characteristic and generation of additional noise.

In spite of a relatively low electric capacitance of the junctions, the McCumber parameter [3] is greater than unity (note fragments of the $I-V$ characteristic with a relatively high differential resistance). Such a result is due to the fact that the connecting lines located above the base electrode behind an insulating layer provide an increase in the effective capacitance of the SQUID Josephson junctions. To decrease such a capacitance, we form slits with a width of 10 μm in the base electrode under the connecting lines and decrease the width of the connecting lines above the

base electrode to 3 μm. Thus, the McCumber parameter decreases to 0.5.

The experiments show resonances of two types in the working interval of the SQUID voltages. The first resonance is the intrinsic LC resonance of the SQUID [11] that corresponds to a voltage of 32 μV (Fig. 3a). The voltage can be increased by a factor of 2 using a decrease in the inductance and capacitance of the SQUID (resonance at 60 μV in Fig. 3b). The second resonance is related to the standing waves in the microstrip line consisting of the base electrode and current lines. The slits that are formed under the connecting lines provide a decrease in the resonator length by a factor of 3, so that the frequencies of the above resonances proportionally increase and leave the working interval of the SQUID. The 3D-MLSI simulation shows that such slits provide an increase in the SQUID inductance by less than 1%, so that the corresponding changes of characteristics are negligible. In addition, a decrease in the width of the parts of connecting lines located above the base electrode leads to both a decrease in the total capacitance of the SQUID and a decrease in the remaining resonances due to mismatch of impedances.

Figure 3b presents the $I-V$ characteristic of the optimized SQUID. It is seen that the McCumber parameter decreases to the optimal level, the resonances are shifted toward higher frequencies, and the intensity of resonances decreases.

3. MEASUREMENT OF THE NOISE CHARACTERISTICS OF THE SQUIDS

We study the noise characteristics of the SQUIDs using the electronic system of [12] that employs the modulation scheme with the negative feedback with respect to magnetic flux and works as a null detector. In the tests of sensors with different topologies, the feedback ranges from 0.6 to 1.2 V/Φ_0 and the level of

intrinsic noise reduced to the input is equivalent to $1\,\mu\Phi_0/\sqrt{Hz}$. For different topologies, the measured values of the rms noise with respect to magnetic flux range from 2.5 to $7\,\mu\Phi_0/\sqrt{Hz}$ (Fig. 4). Such values are sufficient for applications in the NDE systems for diagnostics of materials and metal structures and allow SQUID applications in the magnetocardiographic systems for which the needed resolution with respect to magnetic field is less than $5\,\mu\Phi_0/\sqrt{Hz}$ [13, 14].

Owing to a relatively high sensitivity of the proposed sensors, the resulting noise level of the output voltage depends on the efficiency of shielding of the SQUID sensors with respect to the external interference and the presence of metal elements in the nearest vicinity. The experiments show that a copper stripe with sizes of 1×0.15 mm and a thickness of about 0.05 mm located above the SQUID sensor provides an increase in the output noise level with respect to magnetic flux to $40-50\,\mu\Phi_0/\sqrt{Hz}$.

Fig. 4. Spectral density of the SQUID noise.

4. ENCAPSULATION OF THE SQUID SENSORS

For practical applications of the SQUID sensors, we have developed a setup for connection of microcircuit and external electronic equipment, installation of additional electric components, and protection of the sensor against mechanical damage. In such a setup, the SQUID-sensor chip is fixed on a fiberglass-plastic plate using epoxy adhesive. Then, the contact pads of the bias current and modulation coils are connected with the aid of ultrasonic welding using thin aluminum wire with a diameter of 25 μm to the corresponding contact pads on the board that are connected to the internal part using the PBD-10 2×5 connectors. Twisted-pair wires are connected to the external part of the connector. The corresponding inputs (e.g., plus and minus of the bias currents) are combined in the twisted pairs, so that the sensor becomes more stable against electromagnetic interference in the circuits of control electronics.

The contact pads of the input coil are connected to niobium beads the superconducting electric connection of which to the measurement coil is provided by mechanical pressing of the niobium wire to the bead using an M1.4 screw. Such a system provides simplicity and reliability of the connection of sensor to the measurement setup and interchangeability of the samples.

A resistor with a resistance of 1 kΩ that is used for heating of the sample and a low-pass filter are placed on the fiberglass-plastic plate. The filter consisting of a capacitor with a capacitance of 2.5 nF and a resistor with a resistance of 39 Ω is connected in parallel to the input and measurement coils.

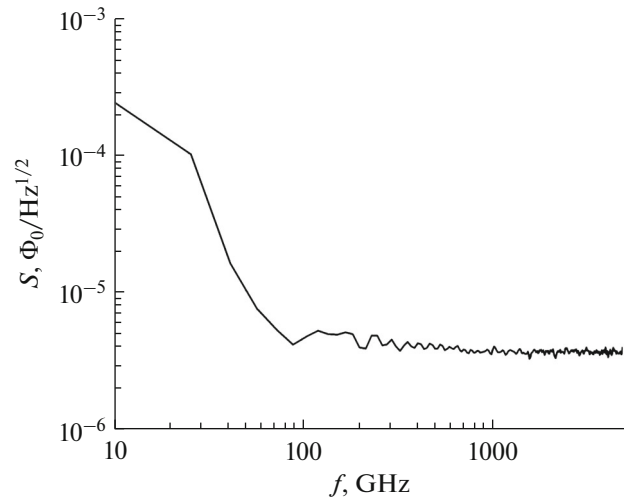The superconducting contact of the external receiving coil and contact pads of the SQUID-sensor chip is an important condition for the practical application of SQUIDs. Such connection is implemented with the aid of additional niobium beads that have superconducting contact with the SQUID input coils. The superconducting contact of the beads and receiving loop is obtained using ultrasonic welding. Such a procedure is difficult to implement for niobium, so that the process has been substantially optimized.

5. OPTIMIZATION OF THE TECHNOLOGY FOR NIOBIUM BONDING

In real magnetometric devices, the magnetic flux in the SQUID passes through the receiving loop with a relatively large diameter that is located outside the sensor and series-connected to the input coil that is inductively coupled to the SQUID loop. To obtain the superconducting contact of the input coil and receiving loop, we have optimized the technology for ultrasonic welding of niobium based on the method of [15].

The main problem of the ultrasonic welding of niobium wire is related to a relatively high rigidity of the material: a standard (for aluminum) pressing of 0.45 N is insufficient for optimal contact area of the wire and surface (niobium layer with a thickness of 300 nm on the SQUID contact pads that is obtained with the aid of the DC magnetron sputtering). The niobium surface is protected against oxidation using a palladium layer with a thickness of 4 nm that does not prevent the formation of the superconducting contact. Normally, the wire is fabricated using the cold drawing, so that significant internal stress is accumulated and the rigidity substantially increases. Vacuum annealing that has been proposed in [15] is used to eliminate internal stress and decrease the rigidity.

The annealing is performed in vacuum with the aid of current flow in the niobium wire with a length of 25 cm. For the annealing, we use a setup that consists of a vacuum chamber, evacuation and pressure-con-

trol system, vacuum current leads, and dc-current (voltage) source. The wire is fixed inside the chamber to avoid damage of the setup in the course of annealing (the temperature of wire may amount to 1500–2000°C). Note the absence of additional electric contacts. The chamber is evacuated to a pressure of about 10^{-6} mbar. The minimum pressure is critically important for the annealing, since an increase in the pressure by a factor of 2 to a level of about 10^{-5} mbar in the course of annealing leads to rapid oxidation of the wire, so that the wire becomes fragile and cannot be used for the ultrasonic welding. The application of a nitrogen trap makes it possible to reach a pressure of 6×10^{-7} mbar at the entrance of the pump system. Such pressure is sufficient for the annealing of wire with a diameter of 25 μm.

Correct annealing makes it possible to obtain substantially softer wire that is not broken upon bending and can be used for the ultrasonic welding. The optimal regimes of the ultrasonic welding depend on several parameters. We use a WestBond 7740 setup for which the best results for a wire with a diameter of 25 μm are obtained at an ultrasonic power of 330, time of 350 ms, and a pressing force of 0.45 N.

CONCLUSIONS

We have optimized the topology of a high-symmetry SQUID to eliminate resonances and, hence, improve the noise characteristics of the sensor. The rms noise with respect to magnetic field for the optimized samples (2.5 $\mu\Phi_0/\sqrt{\mathrm{Hz}}$) allows applications of the SQUID in almost all magnetometric devices. In addition, we have developed technology for ultrasonic welding of niobium that can be useful in technological procedures.

REFERENCES

1. W. G. Jenks, S. S. H. Sadeghi, and J. P. Wikswo, Jr., J. Phys. D: Appl. Phys. **30**, 293 (1997).
2. H. Weinstock, IEEE Trans. Magn. **27**, 3231 (1991).
3. J. Clarke and A. I. Braginski, *The SQUID Handbook: Applications of SQUIDs and SQUID Systems* (Wiley, Hoboken, 2006).
4. M. B. Ketchen and T. J. Watson, IEEE Trans. Magn. **27**, 2916 (1991).
5. M. Ketchen, D. J. Pearson, K. Stawiasz, et al., IEEE Trans. Appl. Supercond. **3**, 1795 (1993).
6. V. P. Koshelets, A. N. Matlashov, I. L. Serpuchenko, et al., IEEE Trans. Magn. **25**, 1182 (1989).
7. M. B. Simmonds, US Patent No. 5053834 (1991).
8. E. A. Kostyurina, K. V. Kalashnikov, L. V. Filippenko, and V. P. Koshelets, Phys. Solid State **58**, 2203 (2016).
9. J. Knuutila, M. Kajola, H. Seppa, et al., J. Low Temp. Phys. **71**, 369 (1988).
10. L. V. Filippenko, S. V. Shitov, P. N. Dmitriev, et al., IEEE Trans. Appl. Supercond. **11**, 816 (2001).
11. K. Enpuku, R. Cantor, and H. Koch, J. Appl. Phys. **72**, 1000 (1992).
12. E. V. Burmistrov, V. Yu. Slobodchikov, V. V. Khanin, Yu. V. Maslennikov, and O. V. Snigirev, J. Commun. Technol. Electron. **53**, 1259 (2008).
13. V. Schultze, R. Stolz, R. Ijsselsteijn, et al., IEEE Trans. Appl. Supercond. **7**, 3473 (1997).
14. Y. V. Maslennikov, M. A. Primin, V. Y. Slobodchikov, et al., Phys. Procedia. **36**, 88 (2012).
15. W. Jaszczukt, H. J. M. ter Brake, J. Flokstra, et al., Meas. Sci. Technol. **2**, 1121 (1991).

Translated by A. Chikishev